Static Frictional Forces at Crystalline Interfaces

D. J. Diestler*

Department of Agronomy, University of Nebraska−Lincoln, Lincoln, Nebraska 68583-0915

E. Rajasekaran and X. C. Zeng

Department of Chemistry, University of Nebraska−Lincoln, Lincoln, Nebraska 68588

Received: January 31, 1997; In Final Form: April 8, 1997[⊗]

A statistical thermodynamic description of the atomic force microscope is developed and used to compute the force of static friction for a single-atom tip on a hexagonal close-packed substrate surface under constant load in vacuum. The substrate atoms are taken to be independent isotropic harmonic oscillators, and the tip−substrate interaction is taken to be Lennard-Jones (12,6). Movement of the tip is treated as a quasistatic (reversible) process. The force of *static* friction (*i.e.*, the maximum of the component of the force parallel to the direction of movement of the tip) is computed by the Monte Carlo technique for several crystallographic directions (paths) and found to be strongly anisotropic. The frictional force is minimum along a particular path where rows of substrate atoms form a "groove"; it is up to 2 orders of magnitude greater for the path perpendicular to the groove. The dependence of the frictional force on the hardness of the substrate (as measured by the force constant of the substrate harmonic potential) and on temperature was examined for these two extreme paths. For hard substrates the frictional force is nearly linear with load. As the substrate gets softer, or as the temperature increases at fixed hardness, the frictional force declines. The results of the computations are correlated with recent experimental observations on the sliding of nanocrystals of MoO_3 over an MoS_2 substrate.

Introduction

With the advent of atomic force microscopy (AFM)[1,2] the molecular mechanisms of friction and lubrication have come under intensive study in recent years.[3−6] We are concerned in this article especially with the ideal situation where two perfect crystalline surfaces slide over each other. Friction in such a system at the atomic scale was first investigated by Mate *et al.*,[7] who observed that when the basal plane of graphite[7] or mica[8] is rastered beneath a tungsten tip under constant load, the tip undergoes lateral stick−slip movements, reflecting a frictional force that oscillates with the period of the basal-plane lattice. Since sliding seems to take place without plastic deformation or degradation of the substrate, a possible explanation of the relatively large periodic component of the frictional force is that the tip rides atop a flake of the substrate that aligns itself with the underlying substrate lattice, thus giving rise to a strong coherent interaction. Subsequent studies of mica sliding on mica[9] and diamond on diamond[10] also reveal substantial periodic components, as well as anisotropy[9] (*i.e.*, dependence of the frictional force on the direction in which the surfaces slide relative to the crystallographic axes of the substrate). Sheehan and Lieber[11] reported recently "lattice-directed sliding" of well-characterized nanocrystals of MoO_3 on single-crystal MoS_2 substrates. That is, an MoO_3 crystallite can be slid only along certain preferred directions with respect to the unit-cell axes of the substrate. Rows of S atoms in the substrate surface form effective channels (or grooves) in which the surface atoms of the MoO_3, which is tilted laterally with respect to the MoS_2 *a* axis, can slide with extraordinarily low friction. Morita *et al.*[12] have observed two-dimensional stick−slip movement of an Si_3N_4 tip over the (0001) MoS_2 surface, when the substrate is scanned in these preferred directions.

Theoretical studies of the tribological properties of clean crystalline interfaces involve qualitative phenomenological approaches[13−17] as well as quantitative quantum chemical,[18,19] mechanical,[20,21] Brownian dynamics,[22−26] and molecular dynamics[27−30] calculations. These have been reviewed very recently in a volume of *Langmuir*[31] devoted to the proceedings of the latest workshop on tribology.

We report here the results of a model study of *static* friction at the crystalline interface within the framework of statistical thermodynamics. This work represents an extension of our previous study at 0 K.[32] In the normal AFM experiment, the substrate is rastered beneath the tip at rates corresponding to about 10^{-8} Å/ps on a molecular scale, which means that the relative separation and alignment of the tip change negligibly during the course of a practical molecular dynamics simulation. We therefore treat the sliding process as quasistatic or reversible. This approach is in the same spirit as that of Gould *et al.*,[21] except that we have allowed for the possibility of nonzero temperatures. The tip is placed at a sequence of lateral positions along a given crystallographic direction (path) under constant load, the system remaining in thermodynamic equilibrium at all times. It is emphasized that sequential placement does not constitute dynamic sliding; no frictional work (dissipated as heat) is done on the system. For each fixed position of the tip (relative to the substrate) we compute the lateral components of the force on the tip due the substrate. The maximum magnitude of the component lying along the given path is taken as the static frictional force. It is the minimum force that must be applied by an external agent in order to initiate motion of the tip along that path.

Model and Theory

In a strict thermodynamic sense our *system* comprises the dynamic portions of the tip and the substrate, that is, the subset

[⊗] Abstract published in *Advance ACS Abstracts,* May 15, 1997.

S1089-5647(97)00395-7 CCC: $14.00

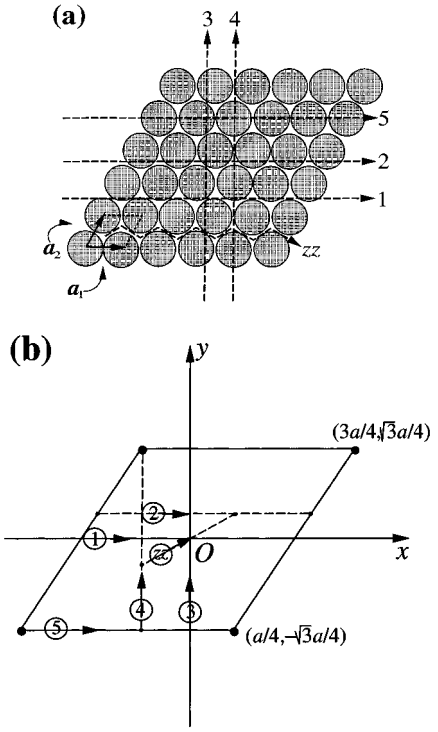

Figure 1. (a) Atomic structure of close-packed substrate, showing several paths of single-atom tip and unit cell of Bravais lattice. (b) Enlargement of unit cell indicating paths of tip and associated unit vectors. Equations of paths are (1) $y = 0$, (2) $y = 3^{1/2}a/12$, (3) $x = 0$, (4) $x = -a/4$, (5) $y = -3^{1/2}a/4$, and (zz) $y = 3^{1/2}x/3$.

of atoms that move with respect to one another according to the classical laws of motion in the field of the *surroundings*, which consist of the *fixed* atoms of the tip and substrate. These fixed atoms make up the "handles" by which the tip and substrate are manipulated. We assume that vacuum intervenes between the tip and the substrate.

The separation and alignment of the tip and substrate are controlled (as external parameters or extensive mechanical variables) by relative movements of the handles. The temperature of the substrate is maintained constant by a thermal bath. For each setting of the handles the system is assumed to be in thermodynamic equilibrium. Reversible transformations are therefore governed by the Gibbs fundamental relation

$$\mathrm{d}A = -S\,\mathrm{d}T - \mathbf{F}\cdot\mathrm{d}\mathbf{r}_\mathrm{t} \tag{1}$$

where A stands for the Helmholtz energy, S for the entropy, T for the absolute temperature, $\mathbf{F}$ for the force on the tip due to the substrate, and $\mathbf{r}_\mathrm{t}$ for position of the tip. The force is given by

$$\mathbf{F} = -(\nabla_{\mathbf{r}_\mathrm{t}} A)_T \tag{2}$$

where $\nabla_{\mathbf{r}_\mathrm{t}}$ signifies the gradient with respect to the tip's position. We take the tip to consist of a *single* atom and the substrate a *single layer* of N hexagonally close-packed atoms (Figure 1). Thus, the *system* comprises just the N-atom layer in the field of the tip. The remainder of the infinite substrate layer makes up the *surroundings*. Periodic boundary conditions are imposed in the directions of the lattice cell vectors $\mathbf{a}_1$ and $\mathbf{a}_2$ (see Figure 1).

The substrate is treated as an Einstein solid, in which each atom vibrates independently in the mean field of its neighbors. The potential energy of the (isolated) substrate is therefore given by

$$U_\mathrm{ss} = \sum_{i=1}^{N} {}^1\!/_2 k(\mathbf{r}_i - \mathbf{r}_{i,0})^2 \tag{3}$$

where $\mathbf{r}_i$ is the instantaneous position of the ith substrate atom, $\mathbf{r}_{i0}$ is its equilibrium position, and k is the common force constant. The tip−substrate interaction is taken to be a pairwise sum

$$U_\mathrm{ts} = \sum_{i=1}^{N} u(r_{it}) \tag{4}$$

of Lennard-Jones (12,6) atomic potentials

$$u(r) = 4\epsilon[(\sigma/r)^{12} - (\sigma/r)^6] \tag{5}$$

where r_{it} is the distance between the tip and ith atom of the substrate. Note that in this case the tip handle coincides with the tip atom, and the substrate handle is the set of N equilibrium positions of the substrate atoms, which are fixed with respect to one another.

In the canonical ensemble, which is naturally suited to the controlled variables T and $\mathbf{r}_\mathrm{t}$, the Helmholtz energy is given by

$$A = -k_\mathrm{B}T \ln Q \tag{6}$$

where k_B is Boltzmann's constant and Q is the canonical partition function, which can be written in the classical limit as

$$Q = Z_N/\Lambda^{3N} \tag{7}$$

The configuration integral Z_N is

$$Z_N = \int \mathrm{d}\mathbf{r}^N \exp[-(U_\mathrm{ss} + U_\mathrm{ts})/k_\mathrm{B}T] \tag{8}$$

where $\mathbf{r}^N$ stands for the collection of $3N$ coordinates and the integration is over all possible $3N$-dimensional configurations of the substrate. The thermal deBroglie wavelength is $\Lambda = (h^2/2\pi m k_\mathrm{B}T)^{1/2}$, m is the mass of the substrate atom, and h is Planck's constant. Combining eqs 2−8, we deduce the following expression for the force on the tip:

$$\begin{aligned}\mathbf{F} &= -\sum_{i=1}^{N} \langle \nabla_{\mathbf{r}_\mathrm{t}} u(r_{it})\rangle \\ &= \sum_{i=1}^{N} \langle \nabla_{\mathbf{r}_i} u(r_{it})\rangle \\ &= -\sum_{i=1}^{N} \langle \mathbf{f}_i\rangle\end{aligned} \tag{9}$$

In eq 9 $\mathbf{f}_i$ is the force on substrate atom i due to the tip and the angular brackets denote the ensemble average, given by

$$\begin{aligned}\langle \mathbf{f}_i\rangle &= -\int \mathrm{d}\mathbf{r}^N Z_N^{-1} \exp[-(U_\mathrm{ss} + U_\mathrm{ts})/k_\mathrm{B}T]\nabla_{\mathbf{r}_i} u(r_{it}) \\ &= -\int \mathrm{d}\mathbf{r}_i \exp\{-[{}^1\!/_2 k(\mathbf{r}_i - \mathbf{r}_{i0})^2 + u(r_{it})]/k_\mathrm{B}T\}\nabla_{\mathbf{r}_i} u(r_{it})/ \\ &\qquad \int \mathrm{d}\mathbf{r}_i \exp\{-[{}^1\!/_2 k(\mathbf{r}_i - \mathbf{r}_{i0})^2 + u(r_{it})]/k_\mathrm{B}T\}\end{aligned} \tag{10}$$

where the second line follows from the separability of the potential energy into a sum of N independent pairwise interactions. Moreover, we note that the force of the tip acting on atom i must be directed along their line of centers. Thus, for convenience, we fix the origin of a "laboratory" coordinate

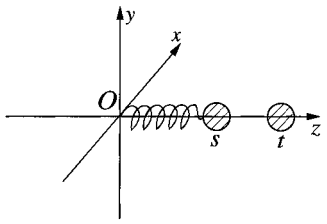

Figure 2. Single harmonically bound substrate atom (s) in field of tip atom (t).

frame at the equilibrium position of the substrate atom and place the tip atom on the positive z axis (see Figure 2). Since the potential energy of the pair is cylindrically symmetric about the z axis, we could in principle employ cylindrical coordinates and reduce the 3-dimensional integral in eq 10 to a 2-dimensional one, which could be effected by two Gaussian quadratures. Although this procedure works for sufficiently high temperature, it fails in the limit of 0 K.

Calculations

The one-atom ensemble average in eq 10 was evaluated by means of the Metropolis Monte Carlo method.[33] In the normal procedure the maximum step size $\delta\mathbf{r}$ is adjusted during the run so that approximately 50% of the trial moves are accepted. However, if the temperature (relative to the changes in the configurational energy, divided by k_B, associated with typical moves) is too low, then $\delta\mathbf{r}$ may be reduced so drastically that the configuration of the system gets stuck. In other words, $\delta\mathbf{r}$ may become so small that the configuration does not change significantly from the initial one in an astronomical number of steps. To avoid this problem, we use the simulated annealing technique,[34,35] in which the initial temperature is reduced to the desired value in stages, so that the configurations are weighted correctly according to the Boltzmann factor. If the desired temperature is T, the initial temperature is T_0, and we employ s stages, then at each stage the temperature of the previous stage is reduced by the factor $(T/T_0)^{1/s}$. At each stage the system is allowed to "equilibrate" for N_s steps. This procedure was verified by setting $T = 10^{-4}\epsilon/k_B$ and observing that the mean displacement of the substrate atom agreed with that determined previously[32] by minimizing the potential energy at $T = 0$ K. For all of the results to be presented here, we set $T_0 = T + \epsilon/k_B$, $s = 10$, and $N_s = 10^5$.

For fixed values of T and the force constant k, we computed the mean force on the tip for equally spaced tip coordinates ranging from 0.1σ to 5.0σ in steps of 0.1σ. Thus, a table of mean force *versus* separation between substrate and tip atoms is generated for the generic pair (see Figure 2). The mean force on the tip at an arbitrary position above the substrate is the (vector) sum of the interpolated pair force over all such pairs whose separations lie within a cutoff radius of 5.0σ.

All quantities are henceforth given in reduced units based on the Lennard-Jones potential: distance is measured in units of the molecular diameter σ; energy is given in units of the well depth ϵ. Thus, forces are measured in units of $\epsilon\sigma^{-1}$ and the force constant in units of $\epsilon\sigma^{-2}$.

Results

The Bravais lattice cell of the substrate is schematized in Figure 1b. For all results to be presented here, the cell constant is set to $a = |\mathbf{a}_1| = |\mathbf{a}_2| = 2^{1/6}\sigma$. The frictional force is computed as a function of path, load, hardness of substrate (force constant, k), and temperature. The tip is moved laterally over the unit cell along the straight line ($y = mx + b$) that specifies the path at fixed load (F_z), force constant, and temperature. In our convention, the *static* frictional force $F_f = |\mathbf{F}\cdot\mathbf{e}|$ for a given path is the maximum *magnitude* of the component of the force acting on the tip in the (lateral) direction of the unit vector $\mathbf{e}$ associated with that path. The load is taken to be the z component of the force applied to the tip.

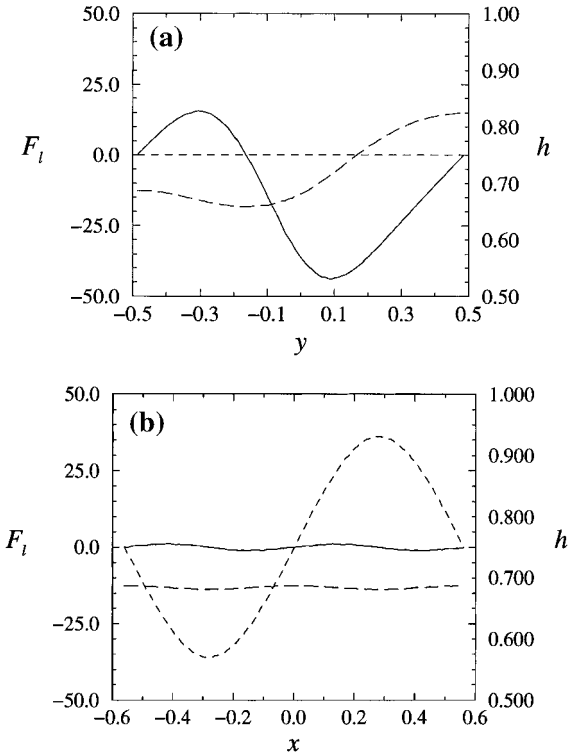

Figure 3. (a) Lateral forces F_x (- - -) and F_y (—) (left ordinate) on tip along path (4) for $k = 10^3$, $F_z = 90$, and $T = 0.0$; distance h (— — —) of tip above equilibrium plane of substrate (right ordinate). (b) Same as (a), except along path (1), F_x (—), F_y (- - -).

Variation of the Lateral Force. Shown in Figure 3 are plots of the lateral components of the force on the tip for paths (1) and (4). Also plotted is h, the altitude of the tip above the equilibrium plane of the substrate. In Figure 1b we see that on path (4) the tip moves parallel to the y axis from $y = -3^{1/2}\,a/4$ (-0.485) to $y = 3^{1/2}a/4$. From physical considerations based on Figure 1 it is clear that F_y vanishes where path (4) intersects the unit-cell boundaries. Also, as the tip is displaced slightly from either boundary, it experiences a force pushing it away from the boundary (*i.e.*, the intersection on either boundary is an unstable point). The plot in Figure 3a, which shows that the slope of F_y is positive at the boundaries, corroborates this. Thus, as the tip is displaced slightly above the lower boundary, it feels a force tending to push it in the $+y$ direction. This force F_y maximizes at $y \sim -0.3$ and then vanishes at $y_{min} \sim -0.15$, the point of globally stable equilibrium. In order to drag the tip to the upper boundary, it is necessary to apply a maximum force (the frictional force) of about 45 to overcome the repulsion of the substrate atom on the boundary, over which the tip finally rests in unstable equilibrium.

Figure 1a indicates that path (4) lies in a reflection plane; by symmetry the contribution to F_x of every atom on the right side of the path is canceled by the equal and opposite contribution of its mirror image. Thus, $F_x = 0$ everywhere on path (4). The variation of the altitude h of the tip above the plane of the substrate is curious. The unstable boundary points correspond to relative maxima in $h(y)$, whereas the stable point y_{min} occurs at the minimum. It appears that the extrema of F_y coincide

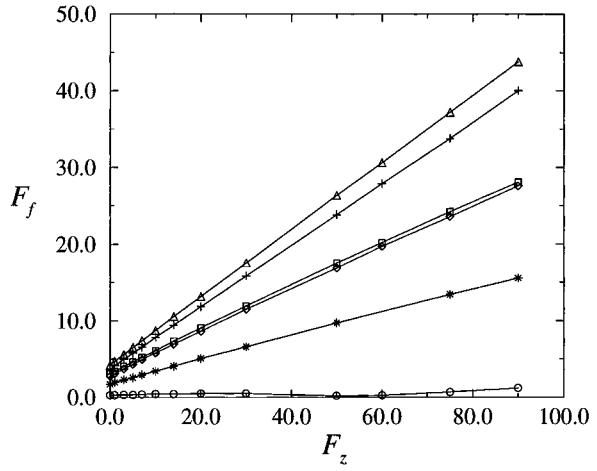

Figure 4. Frictional force F_f *versus* load F_z for paths specified in Figure 1 and $k = 10^3$ and $T = 0.0$. Paths: (1), ○; (2), □; (3), ◇; (4), △; (5) +; (zz), *.

with inflection points in $h(y)$. The stable point occurs at the minimum in the Helmholtz energy (here the internal energy, since $T = 0$ K). The substrate has relaxed to the greatest extent, thus allowing the tip its closest approach.

Again referring to Figure 1, we see that path (1) lies on the x-axis and traverses the unit cell from $x = -a/2$ to $x = a/2$. The relatively low magnitude of F_x (see Figure 3b) indicates that the contribution to F_x due to atoms on either side of path (1) nearly cancel one another, although this is certainly not true for F_y. The unit-cell boundary points are stable for motion in the y-direction, but unstable for motion in the x-direction. The origin, however, is unstable for motion in either direction. Scrutiny of Figure 1 reveals that the force must vanish by symmetry at these points. As the tip is displaced positively along the x axis from the unit-cell boundary point $x = -a/2$ (-0.561), it is strongly repulsed in the y direction by the substrate atom at $(-a/4,3^{1/2}a/4)$. To keep the tip on the x axis, one needs to apply an equal opposing force to the handle. In contrast, a very small force pushes the tip in the x direction toward the stable equilibrium point $x_s \sim -a/4$ (-0.28). Note that F_y is maximum (negative) at x_s, tending to push the tip toward the globally stable trigonal hole. This is also reflected in the relative minimum of $h(x)$ at $(x_s,0)$. To drag the tip on to the origin, where the lateral force vanishes, the maximum force that need be applied in the x direction to the tip, that is, the frictional force, is of the order of only one.

Frictional Anisotropy. Figure 4 displays plots of frictional force *versus* load for the several paths indicated in Figure 1. Along paths (4) and (5), where the tip is required to move directly over substrate atoms, the frictional force is greatest. If the path passes between substrate atoms, as is case for (2) and (3), then we expect F_f to be lower, as indicated in Figure 4. Path (1) passes exactly midway between two rows of substrate atoms, and we see that the frictional force is minimum. The frictional force is actually about 2 orders of magnitude less on path (1) than on either path (4) or (5). Moreover, F_f is approximately independent of load on path (1). Although difficult to observe on the scale of Figure 4, a relative minimum in F_f actually occurs at $F_z \sim 50$. That is, on path (1) F_f actually declines slightly with increasing load in the range $30 < F_z < 50$. It is interesting that, on all paths except (1), the slope of F_f *versus* F_z is approximately constant, decreasing with the distance of the path from substrate atom positions. On the basis of this observation, one might expect the zigzag (zz) path, which passes between trigonal holes and remains as far as possible from substrate atoms, farther in fact than path (1), to offer less frictional resistance than path (1), although Figure 4 gives a contrary indication.

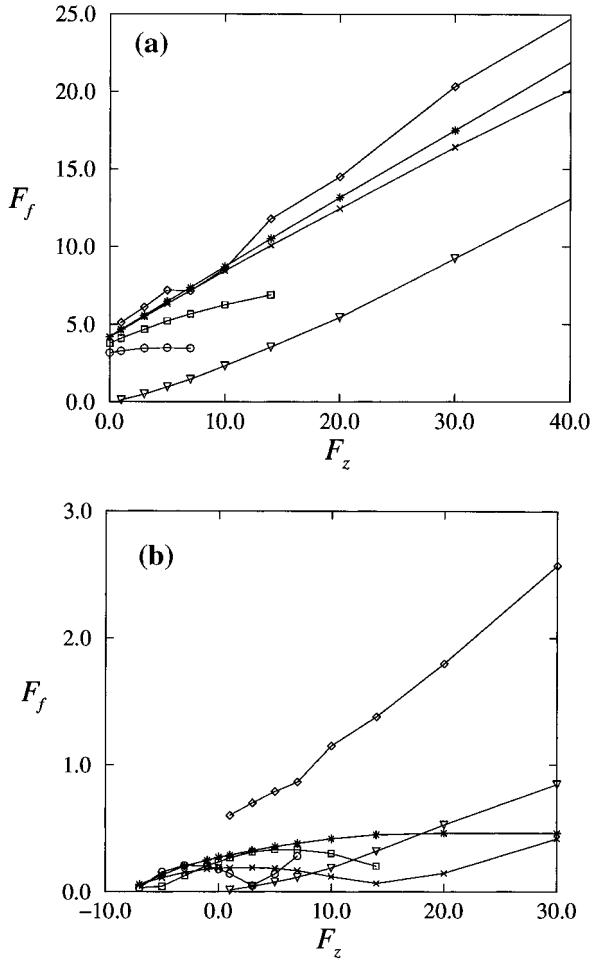

Figure 5. (a) Frictional force F_f *versus* load F_z for path (4) for various hardnesses (k) of substrate at $T = 0.0$. k values: 50, ○; 100, □; 500, ×; 10^3, *; ∞, ◇; ∞ (repulsive term of potential only), ▽. (b) Same as (a), except for path (1).

Some insight into the unique character of path (1) is afforded by the observation that along path (1), where the tip moves exactly midway between two rows of substrate atoms, the atoms in the rows are staggered so that the components of force parallel to the path due to substrate atoms on either side of the path nearly cancel one another. In contrast, on path (zz) the tip must move against two atoms that are precisely opposite each other on either side of the path. Consequently, the components of force parallel to the path due to these two substrate atoms add constructively to oppose the movement of the tip.

Hardness of Substrate. Figure 5 displays plots of frictional force *versus* load for the extreme paths (1) and (4) for various values of the force constant k, which we take to be a measure of the hardness or rigidity of the substrate. The greater the k, the harder the substrate and the higher the frictional force, at least for path (4). This trend can be rationalized in the following way: as k increases, the substrate atoms become more tightly bound to their equilibrium positions, and consequently they can less easily move out of the way of the tip. Again, path (1) is anomalous in this regard, in that for softer substrates the plots exhibit maxima. When the substrate is made rigid ($k = \infty$), so that no relaxation can take place, then the frictional force is greater at all loads. Apparently, relaxation of the substrate lowers the frictional force. Moreover, since the rigid-substrate curves exhibit no maxima, the above-mentioned maxima in the plots for path (1) must somehow be due to relaxation of the

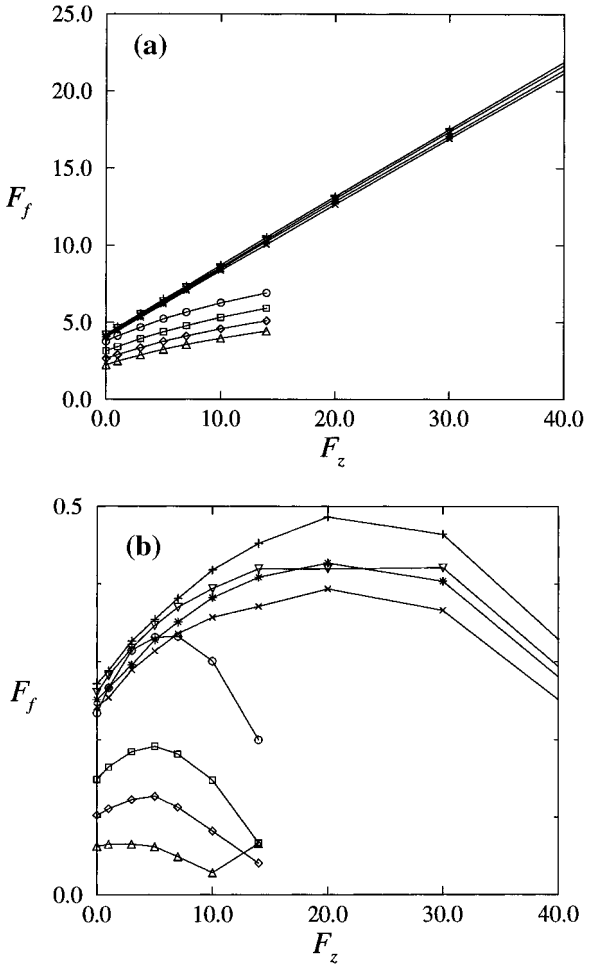

Figure 6. (a) Friction force F_f *versus* load F_z for path (4) for various temperatures (T) and two hardnesses (k) of substrate. $k = 100$: $T = 0.0$, ○; $T = 0.50$, □; $T = 1.00$, ◇; $T = 1.50$, △. $k = 10^3$: $T = 0.0$, +; $T = 0.50$, ∇; $T = 1.00$, *; $T = 1.50$, ×. (b) Same as (a), except for path (1).

substrate. Also plotted in Figure 5 is F_f *versus* F_z for the situation where the substrate is rigid, and only the repulsive term of the Lennard-Jones (12,6) tip−substrate potential is taken into account. The frictional force is uniformly lower than when the full interaction is operative. Over the range $0 < F_z < 10$, F_f is even less than in cases where the substrate can relax. This anti-intuitive result can be explained as follows. With the attraction absent, the tip is not pulled as close to the substrate, so that it does not encounter the substrate atoms as closely in the course of its lateral movement. The attractive part of the tip−substrate potential clearly plays a crucial role in determining the frictional force.

Thermal Effects. Figure 6 shows plots of F_f *versus* F_z on paths (1) and (4) for substrates at several temperatures and two hardnesses. As T increases, F_f decreases. The same trend was observed by Harrison *et al.*[30] in their molecular dynamics study of diamond sliding on diamond. As T increases, the random thermal motion carries substrate atoms farther from their equilibrium positions. The warmer the substrate, the more easily its atoms can move out of the way of the tip. Furthermore, as the substrate gets harder (k increases), the lowering of frictional force due to increased thermal motion is proportionally lessened, as expected.

Discussion

Our calculations demonstrate that the force of *static* friction associated with the movement of a single-atom tip over a close-packed lattice at constant load is extremely anisotropic. Moreover, we find that the tip moves along the particular path (1), where rows of substrate atoms form a "groove", with extremely low friction. The special nature of path (1) is due to the staggering of substrate atoms in adjacent rows, which leads to near cancellation of the components of frictional force arising from alternate substrate atoms. This result is consistent with the recent observation by Sheehan and Lieber[11] of "lattice-directed sliding" of nanocrystals of MoO_3 over single-crystal MoS_2 substrates. In the experiment a silicon nitride tip under fixed load pushes the nanocrystal over the substrate surface. The nanocrystal is found to slide along only three preferred, crystallographically equivalent directions. Although the nanocrystal is polyatomic, Sheehan and Lieber propose that it adjusts its orientation relative to the underlying substrate so that its atoms lie in the parallel grooves (along the preferred directions of sliding) formed by the S atoms of the substrate. The lateral force required to initiate lattice-directed sliding is observed[11] to be proportional to the area of the nanocrystal and hence to the number of its atoms. It is therefore tempting to conclude that the nanocrystal's atoms all experience the same force as they are moved coherently through the grooves. Were this the case, then one atom could represent the whole nanocrystal and our model, in which the single-atom tip is the counterpart of one atom of the nanocrystal, would provide a cogent semiquantitative explanation of lattice-directed sliding. However, along any particular groove the nanocrystal's atoms fall at different (relative) locations in the unit cell of the substrate, since their separation in this dimension bears no relation to the unit cell parameter (a) of the substrate. Thus, when one atom experiences an attraction along the groove, its neighbor may be repelled. On balance, the total maximum force on the atoms in a groove is therefore less than the maximum force on any one atom multiplied by the total number of atoms in the groove. As a consequence, our single-atom model overestimates the static frictional force. Nevertheless, the model is useful in suggesting the preferred direction of sliding and in providing a rough upper bound on the force needed to initiate sliding. Furthermore, the model bears another semiquantitative, albeit perhaps fortuitous, relation to the experiment. Sheehan and Lieber[11] observe that a force applied perpendicularly to the preferred sliding direction fails to budge the nanocrystal, even though that force is up to an order of magnitude higher than those capable of lattice-directed sliding. From Figure 4 it can be seen that the frictional force along path (4) (perpendicular to the preferred direction) is at least an order of magnitude greater than that along path (1) (preferred direction) at all loads.

The above discussion assumes implicitly that both the substrate and the nanocrystal are rigid and that the atoms of the crystal move coherently through the grooves along straight lines. However, as indicated in Figure 3b, there is a strong component of force perpendicular to the groove, which would likely cause the nanocrystal to wiggle as it is moved along the groove. This would correspond roughly to the zigzag path of the single-atom tip (see Figure 1). If this view were correct, then one should compute the minimum force along the groove required to sustain sliding along the zigzag path. Calculations along this line are indeed in progress in our laboratory.

Acknowledgment. The authors are grateful to the National Science Foundation and to the Office of Naval Research for support of the work reported here. They are also pleased to acknowledge helpful comments by a referee on the connection between the model and the experiment. Mark D. Gibson prepared some of the figures. Zeng is indebted to Dr. Y. Zhao (Analog Devices, Inc., MA) for helpful discussions.

References and Notes

(1) Binnig, G.; Quate, C. F.; Gerber, Ch. *Phys. Rev. Lett.* **1986**, *56*, 930.

(2) Meyer, E. *Prog. Surf. Sci.* **1992**, *41*, 3.

(3) Singer, I. L., Pollock, H. M., Eds. *Fundamentals of Friction: Macroscopic and Microscopic Processes*; Kluwer: Dordrecht, 1992.

(4) Belak, J. F., Ed. *Nanotribology*, MRS Bullent *18*(5); Materials Research Society: Pittsburgh, PA, 1993.

(5) Bhushan, B.; Israelachvili, J. N.; Landman, U. *Nature* **1995**, *374*, 607.

(6) Persson, B. N. J., Tosatti, E., Eds. *Physics of Sliding Friction*; Kluwer: Dordrecht, 1992.

(7) Mate, C. M.; McClelland, G. M.; Erlandsson, R.; Chiang, S. *Phys. Rev. Lett.* **1987**, *59*, 1942.

(8) Erlandsson, R.; Hadziioannou, G.; Mate, C. M.; McClelland, G. M.; Chiang, S. *J. Chem. Phys.* **1989**, *89*, 5190.

(9) Hirano, M.; Shinjo, K.; Kaneko, R.; Murata, Y. *Phys. Rev. Lett.* **1991**, *67*, 2642.

(10) Germann, G. J.; Cohen, S. R.; Neubauer, G.; McClelland, G. M.; Coulman, D. *J. Appl. Phys.* **1993**, *73*, 163.

(11) Sheehan, P. E.; Lieber, C. M. *Science* **1996**, *272*, 1158.

(12) Morita, S.; Fujisawa, S.; Sugawara, Y. *Surf. Sci. Rep.* **1996**, *23*, 1.

(13) Sokoloff, J. B. *Surf. Sci.* **1984**, *144*, 267.

(14) Sokoloff, J. B. *Phys. Rev. B* **1990**, *42*, 760.

(15) Sokoloff, J. B. *Thin Solid Films* **1991**, *206*, 208.

(16) McClelland, G. M.; Glosli, J. N. *Fundamentals of Friction: Macroscopic and Microscopic Processes*; Singer, I. L., Pollock, H. M., Eds.; Kluwer: Dordrecht, 1992; p 405.

(17) Colchero, J.; Marti, O.; Mylnek, J. *Forces in Scanning Probe Measurements*; Guntherodt, H.-J., Anselmetti, D., Meyer, E., Eds.; Kluwer: Dordrecht, 1995; p 345.

(18) Zhong, W.; Tomànek, D. *Phys. Rev. Lett.* **1994**, *64*, 3054.

(19) Ferrante, J.; Bozzolo, G. *Fundamentals of Friction: Macroscopic and Microscopic Processes*; Singer, I. L., Pollock, H. M., Eds.; Kluwer: Dordrecht, 1992; p 437.

(20) Hirano, M.; Shinjo, K. *Phys. Rev. B* **1990**, *41*, 11837.

(21) Gould, S. A. C.; Burke, K.; Hansma, P. K. *Phys. Rev. B* **1989**, *40*, 5363.

(22) Persson, B. N. J. *Phys. Rev. Lett.* **1993**, *71*, 1212.

(23) Persson, B. N. J. *Phys. Rev. B* **1993**, *48*, 1814.

(24) Persson, B. N. J. *Phys. Rev. B* **1994**, *50*, 4771.

(25) Persson, B. N. J. *J. Chem. Phys.* **1995**, *103*, 3849.

(26) Matsukawa, H.; Fukuyama, H. *Phys. Rev. B* **1994**, *49*, 17286.

(27) Ribarsky, M. W.; Landman, U. *Approaches to the Modeling of Friction and Wear*; Ling, F. F., Pan, C. H. T., Eds.; Springer: New York, 1988; p 159.

(28) Landman, U.; Leudtke, W. D.; Ringer, E. M. *Fundamentals of Friction: Macroscopic and Microscopic Processes*; Singer, I. L., Pollock, H. M., Eds.; Kluwer: Dordrecht, 1992; p 463.

(29) Cieplak, M.; Smith, E. D.; Robbins, M. O. *Science* **1994**, *265*, 1209.

(30) Harrison, J. A.; White, C. T.; Colton, R. J.; Brenner, D. W. *Phys. Rev B* **1992**, *46*, 9700.

(31) Physical and Chemical Mechanisms of Tribology. *Langmuir* **1996**, *12* (19).

(32) Rajasekaran, E.; Zeng, X. C.; Diestler, D. J. *Micro/Nanotribology and its Applications*; NATO ASI Series E 330; Bhushan, B., Ed.; Kluwer: Dordrecht, 1997; p 371.

(33) Allen, M. P.; Tildesley, D. J. *Computer Simulation of Liquids*; Clarendon Press: Oxford, U.K., 1987.

(34) Kirkpatrik, S.; Gelatt, C. D., Jr.; Vecchi, M. P. *Science* **1983**, *220*, 671.

(35) Wille, L. T.; Vennick, J. *J. Phys. A* **1985**, *18*, L419.

(36) Press, W. H.; Teukolsky, S. A.; Vetterling, W. T.; Flannery, B. P. *Numerical Recipes in Fortran: The Art of Scientific Computing*; Cambridge University Press: Cambridge, U.K., 1992.